Lagrangian trajectories of three-dimensional Rayleigh-Bénard convection

Ambrish Pandey and Jörg Schumacher
Technische Universität Ilmenau, Ilmenau 98693, Germany

1 Introduction

Turbulent convection in horizontally extended domains exhibits regular patterns, known as *turbulent superstructures of convection* [1, 2, 3, 4]. They are similar to those observed near the onset of convection [5, 6]. Rayleigh-Bénard convection (RBC) is an idealized model of thermal convection in which a fluid layer placed between two horizontal plates is heated from below and cooled from above [7]. Crucial parameters governing the dynamics of RBC are the Rayleigh number, the Prandtl number, and the aspect ratio. The Rayleigh number (Ra) signifies the strength of thermal driving force compared to dissipative forces. The Prandtl number (Pr) is the ratio of the time scales of heat and momentum diffusion processes. The aspect ratio (Γ) is the ratio of the width and the height of the convective system. Turbulent heat and momentum transports, which are respectively quantified using the Nusselt and Reynolds numbers, are important response parameters of RBC [7].

We study RBC in a closed rectangular box of dimensions 16:16:1 and compare the characteristic spatial and temporal scales of turbulent superstructures determined in both the Eulerian and Lagrangian frames [8]. We find that the characteristic scales determined using Lagrangian trajectories of the seeded particles in the flow [8] are consistent with those determined in the Eulerian frame of reference [3].

2 Governing Equations

Conservation of mass, momentum, and internal energy lead to equations which govern the dynamics of RBC. In the Boussinesq approximation [7] they are given by

$$\frac{\partial \boldsymbol{u}}{\partial t} + \boldsymbol{u} \cdot \nabla \boldsymbol{u} = -\frac{\nabla p}{\rho_0} + \alpha g (T - T_0)\hat{z} + \nu \nabla^2 \boldsymbol{u}, \tag{1}$$

$$\frac{\partial T}{\partial t} + \boldsymbol{u} \cdot \nabla T = \kappa \nabla^2 T, \tag{2}$$

$$\nabla \cdot \boldsymbol{u} = 0, \tag{3}$$

where $\boldsymbol{u} = (u_x, u_y, u_z)$, T, and p are the velocity, temperature, and pressure fluctuation fields, respectively. Quantities α, ν, κ are thermal expansion coefficient, kinematic viscosity, and thermal diffusivity of the fluid, respectively. Quantities ρ_0 and T_0 denote reference values of mass density and temperature. The acceleration due to gravity g points downward, i.e., in $-\hat{z}$ direction.

The aforementioned equations still carry physical dimensions. However it is convenient to study nondimensional equations. To nondimensionalize the above equations, we use the following transformation:

$$\boldsymbol{x} \rightarrow \tilde{\boldsymbol{x}} = \frac{\boldsymbol{x}}{H} \tag{4}$$

$$\boldsymbol{u} \rightarrow \tilde{\boldsymbol{u}} = \frac{\boldsymbol{u}}{u_f} \tag{5}$$

$$t \rightarrow \tilde{t} = \frac{t u_f}{H} \tag{6}$$

$$T \rightarrow \tilde{T} = \frac{T}{\Delta T}, \tag{7}$$

$$p \rightarrow \tilde{p} = \frac{p}{\rho_0 u_f^2}. \tag{8}$$

Here H is the distance between two horizontal plates or the height of the box and $\Delta T (= T_{\text{bottom}} - T_{\text{top}} > 0)$ is the temperature difference between them. Time is measured in units of the free-fall time $T_f = H/u_f$, and velocities are given in units of the free-fall velocity, $u_f = \sqrt{\alpha g \Delta T H}$. The nondimensional RBC equations are

$$\frac{\partial \tilde{\boldsymbol{u}}}{\partial \tilde{t}} + \tilde{\boldsymbol{u}} \cdot \tilde{\nabla} \tilde{\boldsymbol{u}} = -\tilde{\nabla} p + \tilde{T} \hat{z} + \sqrt{\frac{Pr}{Ra}} \tilde{\nabla}^2 \tilde{\boldsymbol{u}}, \tag{9}$$

$$\frac{\partial \tilde{T}}{\partial \tilde{t}} + \tilde{\boldsymbol{u}} \cdot \tilde{\nabla} \tilde{T} = \frac{1}{\sqrt{Pr Ra}} \tilde{\nabla}^2 \tilde{T}, \tag{10}$$

$$\tilde{\nabla} \cdot \tilde{\boldsymbol{u}} = 0. \tag{11}$$

Two nondimensional parameters appear in above equations, which are the main governing parameters of RBC. The Rayleigh and Prandtl numbers are defined as

$$Ra = \frac{\alpha g \Delta T H^3}{\nu \kappa}, \tag{12}$$

$$Pr = \frac{\nu}{\kappa}. \tag{13}$$

From now on we drop the tilde.

3 Numerical Method

We solve the governing equations [Eqs. 9–11] in a rectangular box with $L_x = 16, L_y = 16, H = 1$ using a spectral element solver NEK5000 [9], which has been adapted to our specific requirements [10]. We study the turbulent convection in air ($Pr = 0.7$) at a moderate Rayleigh number $Ra = 10^5$. The no-slip condition, i.e., $\boldsymbol{u} = 0$, is employed on all the boundaries. For the temperature field, the isothermal boundary condition (i.e., $T =$ constant) is applied at the top and bottom plates. At the sidewalls, adiabatic or perfectly thermally insulated condition is employed, where the normal derivative vanishes, i.e., $\partial T/\partial n = 0$.

The computational domain is divided into 440,896 spectral elements, and each element is further refined by using the Legendre polynomials upto 5th order in each direction. Thus, we simulate our convection flow with 55 million nonuniform grid points. After the flow has reached a statistically steady state, 512^2 uniformly distributed Lagrangian tracer particles are seeded in the flow near the bottom plate at $z = 0.03$. The tracer particles are then advected in the flow according to

$$\frac{d\boldsymbol{X}_i}{dt} = \boldsymbol{u}(\boldsymbol{X}_i, t), \tag{14}$$

where $\boldsymbol{X}_i$ is the position of i^{th} tracer particle. Interpolation of the velocity field at nongrid locations is performed using a highly accurate spectral interpolation method.

4 Results and data structure

The temperature field in midplane is exhibited in figure 1. Turbulent superstructures are visible in the form of hot upwelling and cold downwelling fluids [3].

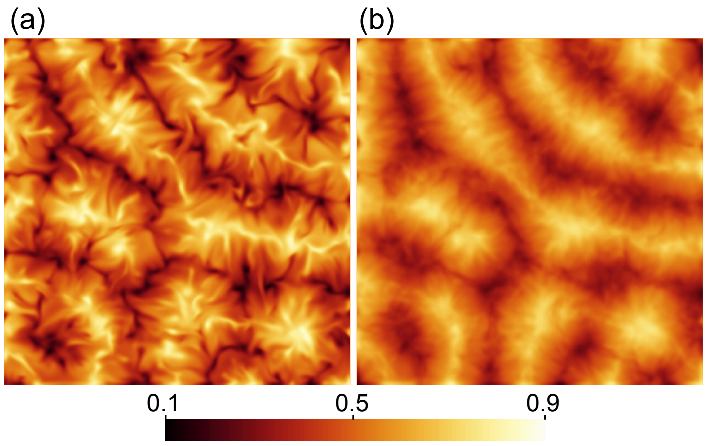

Figure 1: Instantaneous (a) and time-averaged (b) temperature field in midplane exhibiting superstructures in the form of hot upwelling and cold downwelling fluids.

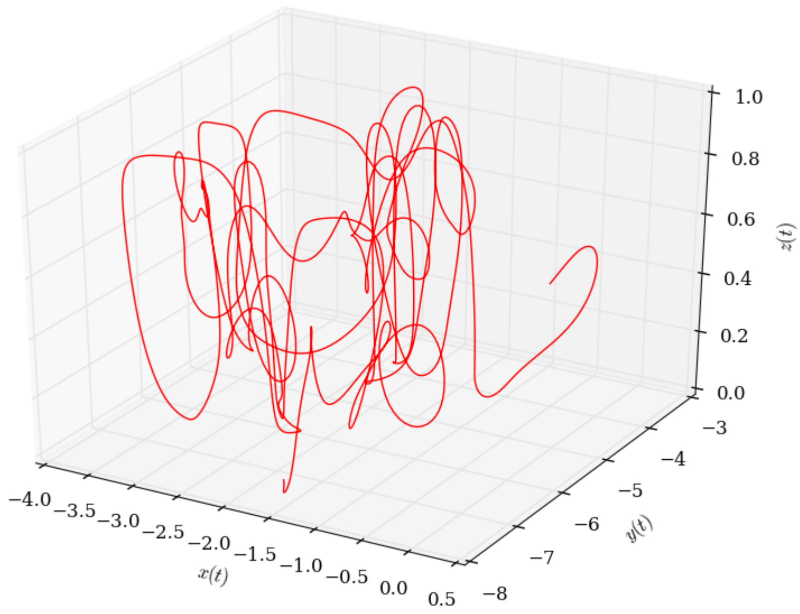

Figure 2: Typical trajectory of a tracer particle during the 235.8 convective time units. The trajectory does not always follow the superstructure rolls, and sometimes trapped in the center.

The position of each Lagrangian tracer is stored at every $0.131\,T_f$ (i.e., every 20 integration time steps) for a total duration of 235.8 T_f. Thus, there are 1801 ASCII files corresponding to each time step, which contain the positions of all the 512^2 tracers, as well as the local convective heat flux along the track. The local heat flux at $\boldsymbol{X}_i(t)$ in the flow is given by

$$Nu(\boldsymbol{X}_i) = 1 + \sqrt{RaPr}\, u_z(\boldsymbol{X}_i)T(\boldsymbol{X}_i). \tag{15}$$

The trajectory of a representative tracer particle is displayed in figure 2, which shows that the tracer particle does not move up and down regularly. Instead, it moves in an irregular fashion between top and bottom plates, sometimes being trapped in the center. Other Lagrangian tracers exhibit similar trajectories.

References

[1] T. Hartlep, A. Tilgner, and F. H. Busse, "Large scale structures in Rayleigh-Bénard convection at high Rayleigh numbers," *Phys. Rev. Lett.*, vol. 91, p. 064501, Aug 2003.

[2] M. S. Emran and J. Schumacher, "Large-scale mean patterns in turbulent convection," *J. Fluid Mech.*, vol. 776, pp. 96–108, 2015.

[3] A. Pandey, J. D. Scheel, and J. Schumacher, "Turbulent superstructures in Rayleigh-Bénard convection," *Nat. Commun.*, vol. 9, p. 2118, May 2018.

[4] R. J. A. M. Stevens, A. Blass, X. Zhu, R. Verzicco, and D. Lohse, "Turbulent thermal superstructures in Rayleigh-Bénard convection," *Phys. Rev. Fluids*, vol. 3, p. 041501, Apr 2018.

[5] M. C. Cross and P. C. Hohenberg, "Pattern formation outside of equilibrium," *Rev. Mod. Phys.*, vol. 65, pp. 851–1112, Jul 1993.

[6] E. Bodenschatz, W. Pesch, and G. Ahlers, "Recent developments in Rayleigh-Bénard convection," *Annu. Rev. Fluid Mech.*, vol. 32, no. 1, pp. 709–778, 2000.

[7] F. Chillà and J. Schumacher, "New perspectives in turbulent Rayleigh-Bénard convection," *Eur. Phys. J. E*, vol. 35, p. 58, 2012.

[8] C. Schneide, A. Pandey, K. Padberg-Gehle, and J. Schumacher, "Probing turbulent superstructures in Rayleigh-Bénard convection by lagrangian trajectory clusters," *Phys. Rev. Fluids*, vol. 3, p. 113501, Nov 2018.

[9] P. F. Fischer, "An overlapping schwarz method for spectral element solution of the incompressible Navier-Stokes equations," *J. Comp. Phys.*, vol. 133, no. 1, pp. 84–101, 1997.

[10] J. D. Scheel, M. S. Emran, and J. Schumacher, "Resolving the fine-scale structure in turbulent Rayleigh-Bénard convection," *New J. Phys.*, vol. 15, p. 113063, 2013.